Juno Magnetometer Observations at Ganymede: Comparisons With a Global Hybrid Simulation and Indications of Magnetopause Reconnection

Norberto Romanelli, G. A. Dibraccio, Ronan Modolo, Jack E. P. Connerney, R. W. Ebert, Y. Martos, T. Weber, J. R. Espley, W. S. Kurth, F. Allegrini, et al.

Geophysical Research Letters

RESEARCH LETTER
10.1029/2022GL099545

Special Section:
Results from Juno's Flyby of Ganymede

Juno Magnetometer Observations at Ganymede: Comparisons With a Global Hybrid Simulation and Indications of Magnetopause Reconnection

N. Romanelli[1,2], G. A. DiBraccio[2], R. Modolo[3], J. E. P. Connerney[2,4], R. W. Ebert[5,6], Y. M. Martos[1,2], T. Weber[2,7], J. R. Espley[2], W. S. Kurth[8], F. Allegrini[5,6], P. Valek[5,6], and S. J. Bolton[5]

[1]Department of Astronomy, University of Maryland, College Park, MD, USA, [2]Planetary Magnetospheres Laboratory, NASA Goddard Space Flight Center, Greenbelt, MD, USA, [3]Laboratoire Atmosphères, Milieux et Observations Spatiales, IPSL, CNRS, UVSQ, UPMC, Paris, France, [4]Space Research Corporation, Annapolis, MD, USA, [5]Southwest Research Institute, San Antonio, TX, USA, [6]Department of Physics and Astronomy, University of Texas at San Antonio, San Antonio, TX, USA, [7]Department of Physics and Astronomy, Howard University, Washington, DC, USA, [8]Department of Physics and Astronomy, University of Iowa, Iowa City, IA, USA

Abstract Juno's flyby of Ganymede on 7 June 2021, provides a unique opportunity to explore the moon's magnetosphere. By means of Magnetometer (MAG) observations and a hybrid numerical simulation, we provide a global description of this environment and analyze the upstream magnetopause in detail. In particular, LATMOS Hybrid Simulation results suggest Juno observed open (one foot-point connected to Ganymede, the other to Jupiter) and closed magnetic field lines along its trajectory. Additionally, we determine that the upstream magnetopause location and orientation seen by Juno MAG are consistent with previous Galileo observations. We observe a non-zero normal component of the magnetic field across the magnetopause, along with flux rope structures embedded within the boundary's current sheet. Both signatures are strong indicators that magnetic reconnection was occurring along Ganymede's magnetopause. Based on this crossing, we calculate a shear angle of ~78° across the magnetopause, with a dimensionless reconnection rate of ~0.12.

Plain Language Summary In this work we provide a global description of Ganymede's magnetosphere in the context of Juno's flyby and investigate one of its main magnetospheric boundaries, the upstream magnetopause. This is done by analyzing magnetic field observations and performing a hybrid numerical simulation. In particular, we find that the upstream magnetopause position and orientation seen by Juno Magnetometer are consistent with observations from the previous Galileo mission. We also find and investigate strong indicators of magnetic reconnection occurring along Ganymede's magnetopause, a physical process where magnetic energy is converted to kinetic and thermal energy, and particle acceleration.

Key Points:

- LATMOS hybrid numerical simulation provides a global description of Ganymede's magnetosphere in the context of Juno's flyby
- We find the upstream magnetopause location and orientation based on Juno Magnetometer data are consistent with previous Galileo observations
- The non-zero magnetic field normal component across the magnetopause and detection of flux ropes are indicators of magnetic reconnection

Correspondence to:
N. Romanelli,
norberto.romanelli@nasa.gov

Citation:
Romanelli, N., DiBraccio, G. A., Modolo, R., Connerney, J. E. P., Ebert, R. W., Martos, Y. M., et al. (2022). Juno Magnetometer observations at Ganymede: Comparisons with a global hybrid simulation and indications of magnetopause reconnection. *Geophysical Research Letters*, *49*, e2022GL099545. https://doi.org/10.1029/2022GL099545

Received 11 MAY 2022
Accepted 28 JUL 2022

1. Introduction

Ganymede is the largest moon in our solar system and the only moon known to possess an intrinsic magnetic field (Kivelson et al., 1996). This intrinsic field is mainly dipolar, with an axis that is tilted by ~176° from Ganymede's spin axis, and an equatorial surface dipole strength of ~719 nT (Gurnett et al., 1996; Kivelson et al., 1996, 2002). Orbiting around Jupiter at an average distance of 14.97 R_J (1 R_J = 71,492 km), Ganymede's mini-magnetosphere is located inside Jupiter's magnetosphere and interacts with the magnetized sub-Alfvénic and subsonic Jovian plasma flow. As a result, Jupiter's magnetic field compresses Ganymede's intrinsic magnetic field on the upstream side, creating a magnetopause (e.g., Kivelson et al., 1998). Magnetic field lines inside Ganymede's magnetosphere near the upstream equator are closed (both foot-points connected to the moon) and approximately anti-parallel to the local Jovian magnetic field, suggesting magnetic reconnection is a major process for plasma dynamics in this system (e.g., Collinson et al., 2018; Kaweeyanun et al., 2020; Tóth et al., 2016; Zhou et al., 2020). In contrast, magnetic field lines in the large polar caps of Ganymede are open (one foot-point connected to Ganymede and the other to Jupiter's ionosphere), facilitating particle precipitation and escape (e.g., Carnielli et al., 2020b). Globally, Ganymede's magnetosphere possesses a cylindrical shape, extended Alfvén wings, and lacks a bow shock preceding the upstream magnetopause (e.g., Jia et al., 2008, 2010).

Ganymede's upstream magnetopause has been studied through data analysis, and theoretical and numerical modeling. The Galileo mission has revealed that this boundary is characterized by sudden rotations in the magnetic field orientation and rapid changes in the plasma properties (e.g., Kivelson et al., 1996; Williams et al., 1997). The identification of magnetopause crossings has also permitted analytical modeling of Ganymede's magnetosphere and to explore the capabilities and limitations of several models, for instance, the so-called superposition model (Kivelson et al., 1998). In particular, the magnetopause model implemented by Kivelson et al. (1998) described the magnetosphere as a cylinder with an elliptical cross section, where the offset of its center is a function of the external Jovian magnetic field orientation, among other parameters. Based on this model, Kaweeyanun et al. (2020) assessed the conditions that are favorable for magnetic reconnection at Ganymede's upstream magnetopause. The authors concluded that reconnection can occur at any location where Ganymede's closed magnetic field lines interact with Jupiter's local magnetic field and that multiple X-lines and widespread flux transfer events are potentially present there. Furthermore, numerical simulations play a crucial role in allowing us to better understand Ganymede's magnetosphere, especially since there are relatively few observations. In this context, Magnetohydrodynamics (MHD), resistive MHD, Hall-MHD, multi-fluid and, to a lesser degree, hybrid numerical simulations have been performed to describe and investigate Ganymede's magnetosphere and to put spacecraft measurements into context (e.g., Dorelli et al., 2015; Fatemi et al., 2016; Jia & Kivelson, 2021; Jia et al., 2008, 2010; Paty & Winglee, 2004, 2006). In particular, MHD simulations suggest that intermittent magnetic reconnection signatures are present across large regions of the magnetopause of Ganymede (Jia et al., 2010). Investigations describing magnetic reconnection at Ganymede's magnetosphere at smaller spatial and temporal scales can be found in, for example, Dorelli et al. (2015), Tóth et al. (2016), and Zhou et al. (2020).

After nearly 20 years since the end of the Galileo mission, Juno's flyby of Ganymede offers a distinct opportunity to improve the current understanding of the mini-magnetosphere (Bolton et al., 2017). In this work, we analyze Juno Magnetometer (MAG) observations focusing on Ganymede's upstream magnetopause and perform a LATMOS hybrid numerical simulation (LatHyS) to provide a global description during this flyby (Connerney et al., 2017; Modolo et al., 2016).

2. Juno MAG and LatHyS Model

Juno MAG measures vector magnetic fields at a maximum sampling rate of 64 Hz, which is analyzed here (Connerney, 2017; Connerney et al., 2017). LatHyS is a global three-dimensional hybrid model that allows to investigate plasma processes occurring in the magnetospheres of Mercury (Richer et al., 2012), Mars (Modolo et al., 2005, 2006, 2012, 2016, 2018; Romanelli, Modolo, Leblanc, Chaufray, Martinez, et al., 2018; Romanelli, Modolo, Leblanc, Chaufray, Hess, et al., 2018; Romanelli et al., 2019), Titan (Modolo et al., 2007), and Ganymede (Leclercq et al., 2016). The reader is referred to Modolo et al. (2016) for a detailed description of this model. Juno MAG data and simulation results are presented in the Ganymede centered Phi-Omega (GPhiO) coordinate system, defined by the following axes: X points along the incident Jovian flow direction, Y is directed along Ganymede-Jupiter vector (positive toward Jupiter), and Z is parallel to Jupiter's spin axis.

In this work, we have performed a stationary hybrid simulation, following a simplified approach. The simulation box has $182 \times 306 \times 306$ cells, and a uniform spatial resolution equal to ∼244 km, that is, half the Jovian plasma ion inertial length (∼487 km). We consider the background Jovian plasma wind around Ganymede is made of oxygen ions (O^+), has temperature equal to ∼250 eV and a mean speed of 140 km s^{-1} along the X-axis (Dougherty et al., 2017; Fatemi et al., 2016; Kim et al., 2020). The total Jovian wind electron density is defined equal to ∼3.5 cm^{-3}, that is, near the lower limit observed by Juno Jovian Auroral Distributions Experiment (JADE) along this flyby (∼4 cm^{-3}) and close to the average number density near Ganymede's orbit (Allegrini et al., 2022; Kivelson et al., 2004; McComas et al., 2017). The background magnetic field is set equal to (−15.4, 40.1, −80.9) nT, as seen by MAG along the outbound leg of the flyby. Thus, the Jovian wind Alfvén Mach number is ∼0.52. For simplicity, Ganymede's ionosphere is assumed to be spherically symmetric, made of O^+ ions, with a surface density and scale height equal to 500 cm^{-3} and 125 km, respectively (Eviatar et al., 2001; Paty et al., 2008). Ganymede's magnetic field is described through the intrinsic dynamo dipolar field reported in Kivelson et al. (2002). The results presented in this Letter correspond to simulation time equal to 300 $\Omega_{O^+}^{-1} \sim 543$ s ($\Omega_{O^+}^{-1}$ is the inverse of the O^+ ion gyrofrequency), where we consider the system to be stationary.

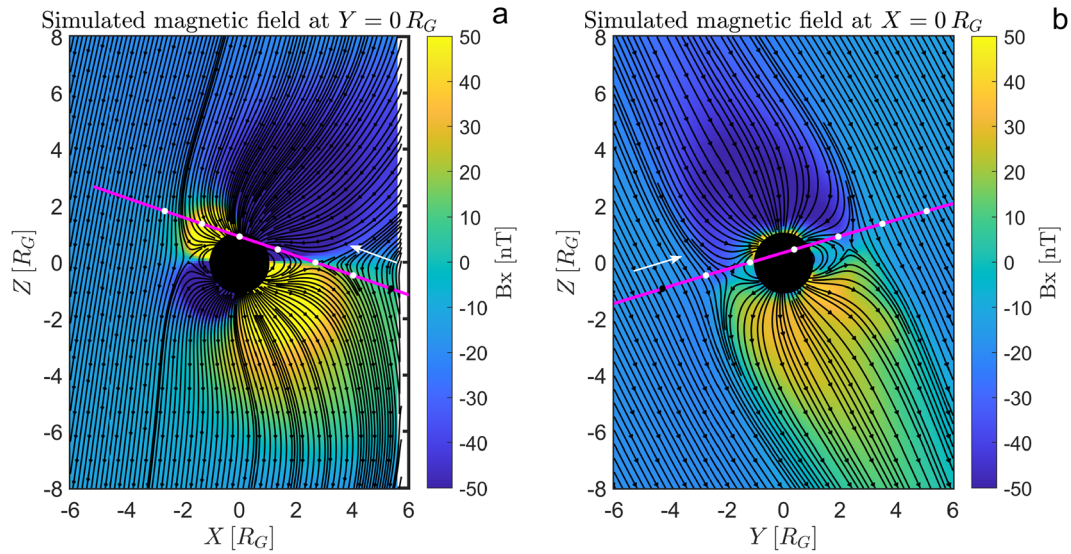

Figure 1. Simulated magnetic field Bx (Ganymede centered Phi-Omega) component at the $Y = 0\ R_G$ (panel a) and $X = 0\ R_G$ (panel b). Field lines (shown in black) are computed based on the magnetic field components contained in each of these planes. Juno's trajectory projections are shown by the magenta solid lines and the six dots show its location between 16:40 UT (black dot) and 17:10 UT, separated by 5 min intervals. The white arrows indicate the direction of increasing time.

3. Results and Discussion

3.1. Global Description of Ganymede's Magnetosphere

Figure 1 displays the simulated Bx component (color coded) as a function of X and Z (panel a) and Y and Z (panel b). In particular, this figure shows the main regions and boundaries in Ganymede's magnetosphere: the Alfvén wings, the magnetopause boundary separating Jovian magnetic field lines (both ends at Jupiter's ionosphere) from open lines (one end at Jupiter's ionosphere and the other at Ganymede) as well as a region of closed magnetic field lines. Juno's Ganymede flyby took place with the spacecraft moving from the wake region (relative to the Jovian co-rotational flow) toward the upstream side and from the anti-Jovian side toward Jupiter.

Figures 2a–2d display Juno MAG observations (in blue) and the LatHyS simulated profiles (in red) along the spacecraft trajectory between 16:40 and 17:10 UT. The LatHyS profiles are derived by linearly interpolating simulated values at simulation cells adjacent to the spacecraft trajectory (trilinear interpolation method). For completeness, these panels also present the magnetic field profiles associated with the so-called superposition model (in black), computed as the linear combination between Ganymede's dipolar field and the Jovian magnetic field seen by Juno (Kivelson et al., 1998). For this, we set the Jovian magnetic field equal to (−15.4, 40.1, −80.9) nT (based on MAG observations along the outbound leg of the flyby) and consider Ganymede's intrinsic field reported in Kivelson et al. (2002). Initially, Juno observes Jupiter's magnetic field, oriented mainly along the−Z-axis, with a magnitude of ∼65 nT. At ∼16:43 UT, Juno measured variability in the magnetic field as the field changed direction and decreased in magnitude, suggesting the spacecraft entered into the wake region, affected by the presence of Ganymede's intrinsic field (Hansen et al., 2022). MAG measurements display significant magnetic field fluctuations and weaker field strength until ∼16:50 UT, when Juno likely reached Ganymede's magnetopause (Allegrini et al., 2022; Clark et al., 2022; Duling et al., 2022; Kurth et al., 2022; Weber et al., 2022).

MAG measurements also show Juno visited the northern region of Ganymede's Alfvén wings, partly characterized by negative local Bx and By components (Figures 2a and 2b). The spacecraft's closest approach to Ganymede (∼1,046 km from the surface) occurred at ∼16:56:08 UT (Figure 2e, left vertical axis). We identify a rotation in the magnetic field between ∼17:00:39.24 UT and ∼17:01:05.52 UT (see vertical dash lines, panels 2a–2d), as the field magnitude decreased. These features are indicative of Juno's upstream magnetopause crossing of Ganymede along the outbound leg, in agreement with conclusions from plasma and waves observations (e.g., Allegrini et al., 2022; Ebert et al., 2022; Kurth et al., 2022). Hereafter, the times identified as the beginning and

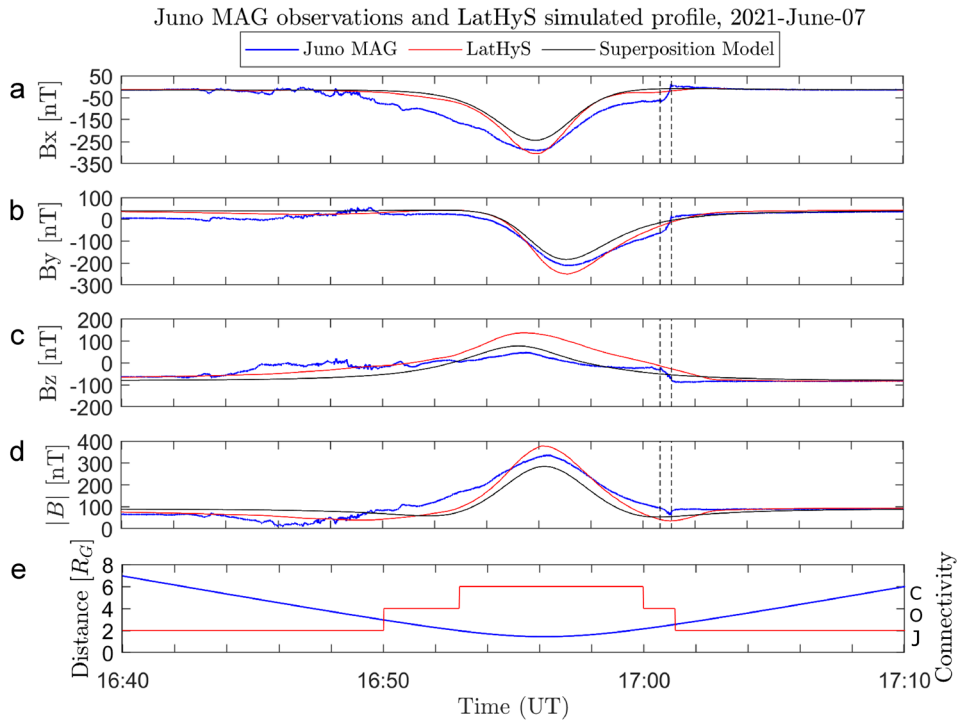

Figure 2. Panels (a–d): Juno 64 Hz Magnetometer observations (in blue), LATMOS hybrid numerical simulation (in red) and the superposition model (in black) profiles along the spacecraft trajectory (in Ganymede centered Phi-Omega coordinates) as a function of time. Vertical dashed lines mark the beginning and end of Juno's upstream Ganymede's magnetopause crossing. Panel (e) (left) Juno distance to Ganymede's center (in blue), (right) simulated connectivity of the magnetic field lines along Juno trajectory. C, O, and J correspond to closed, open, and Jovian magnetic field lines (in red).

end of this outbound magnetopause (MP) boundary crossing are referred to as MP t_1 (~17:00:39.24 UT) and MP t_2 (~17:01:05.52 UT), respectively.

Figures 2a–2d also shows there is a limited agreement between Juno MAG observations and magnetic field profiles derived from LatHyS and the superposition model. Although LatHyS reproduces the Bx and By magnetic field components more accurately, the superposition model better represents the Bz component. Discrepancies near closest approach (Bz component) are also present in MHD simulations and may be associated with the inner boundary conditions of these models (Duling et al., 2022). Moreover, some of the observed differences are also likely due to the simplicity of the Jovian plasma wind model and the coarse simulation grid. The limitations of the superposition model are also evident and are on the same order to what was reported for the G8 flyby (Kivelson et al., 1998). Part of the observed differences between model predictions (LatHyS and the superposition) and observations could be due to complex processes occurring near Ganymede's wake and the relatively high-beta plasma environment, associated with the moon's location with respect to Jupiter's plasma sheet during this encounter (e.g., Connerney et al., 2020; Ebert et al., 2022; Hansen et al., 2022).

Figure 2e (right vertical axis) shows the magnetic field connectivity derived from LatHyS along Juno's trajectory (in red). This simulation suggests Juno entered Ganymede's magnetosphere around ~16:50 UT, and visited a region of open magnetic field lines until ~16:53 UT. Thereafter, LatHyS suggests Juno observed closed magnetic field lines until ~17:00 UT, and later, it sampled a region of open magnetic field lines. LatHyS results indicate Juno measures again Jovian magnetic field lines after ~17:01:12 UT. We find that both simulated boundaries separating Jovian from open magnetic field lines are in good agreement with estimations for the magnetopause crossings from JADE and Jovian Energetic Particle Detector Instrument observations. In contrast, these measurements also suggest Juno did not cross into the closed field line region during this flyby (Allegrini et al., 2022; Clark et al., 2022; Mauk et al., 2017; McComas et al., 2017). Some of these differences could be attributed to the likely proximity of Juno's trajectory to the boundary separating open from closed magnetic field lines. We refer the reader to Kurth et al. (2022), Clark et al. (2022), and Duling et al. (2022) for analyses of Juno waves

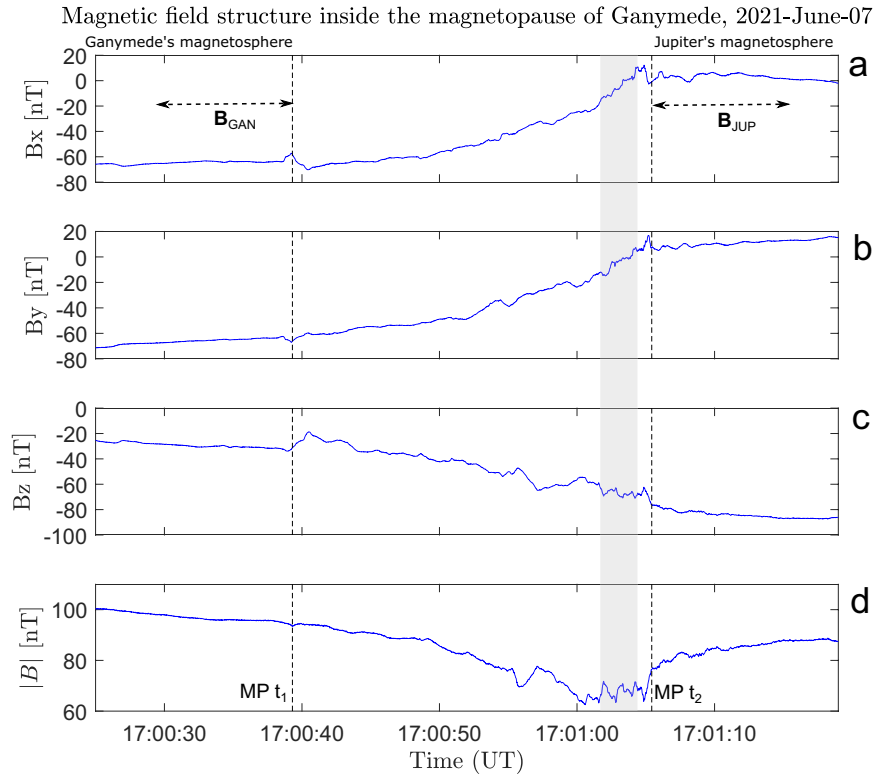

Figure 3. Magnetic field Ganymede centered Phi-Omega components and strength seen by Juno Magnetometer, between 17:00:24 and 17:01:18 UT. Vertical dashed lines mark the beginning (MP t_1 = 17:00:39.24 UT) and end (MP t_2 = 17:01:05.52 UT) of Juno's upstream Ganymede's magnetopause crossing. $\mathbf{B}_{GAN}$ = (−63.82, −65.27, −30.38) nT and $\mathbf{B}_{JUP}$ = (3.61, 10.05, −83.09) nT are the mean magnetic fields between 17:00:29 UT and MP t_1 and between MP t_2 and 17:01:15 UT, respectively. The shaded gray area shows quasi-periodic structures analyzed in Figure 4.

and plasma observations and MHD simulations in this context. Future numerical simulations considering more realistic boundary conditions, for example, ionosphere models (Carnielli et al., 2019, 2020a) may help to better understand this discrepancy. Moreover, a detailed analysis of MAG observations near Juno's closest approach to Ganymede will also shed light on this matter.

Next, we compare Juno MAG observations and the simulation results with predictions, based on Galileo observations. We consider the magnetopause surface function $f(X, Y, Z)$ developed by Kivelson et al. (1998), expressed in GPhiO coordinates in Kaweeyanun et al. (2020). As shown in both studies, $f(X, Y, Z)$ is equal to 1 for any point contained in Ganymede's magnetopause. We compute the expected location for Ganymede's magnetopause associated with the inbound and outbound Jovian magnetic field conditions. By considering the temporal evolution of Juno's location with respect to Ganymede and the moon's system III East longitude, we determine when f is equal to 1. This theoretical model predicts the magnetopause would be observed at 16:50:15 and 17:00:50 UT, if we consider the mean value of these parameters between 16:40 and 16:42:30 UT. Similarly, by considering the Jovian magnetic field observed after MP t_2, we find the magnetopause crossing (f = 1) at 16:50:11 and 17:01:23 UT. In both cases, the predicted inbound magnetopause location is very close to the simulated boundary separating Jovian and open magnetic field lines from LatHyS (Figure 2e), in agreement with Allegrini et al. (2022), Kurth et al. (2022), and Duling et al. (2022). This is also the case for Ganymede's magnetopause location along Juno's outbound leg.

3.2. Magnetic Reconnection at Ganymede's Upstream Magnetopause From Juno MAG

Figure 3 shows the observed magnetic field components and strength as a function of time, between 17:00:24 and 17:01:18 UT. Juno's mean location between MP t_1 and MP t_2 was (−0.22, 2.21, 0.99) R_G, where R_G stands for Ganymede radii (1 R_G ~ 2,634 km). This shows Juno's upstream magnetopause crossing occurred along the

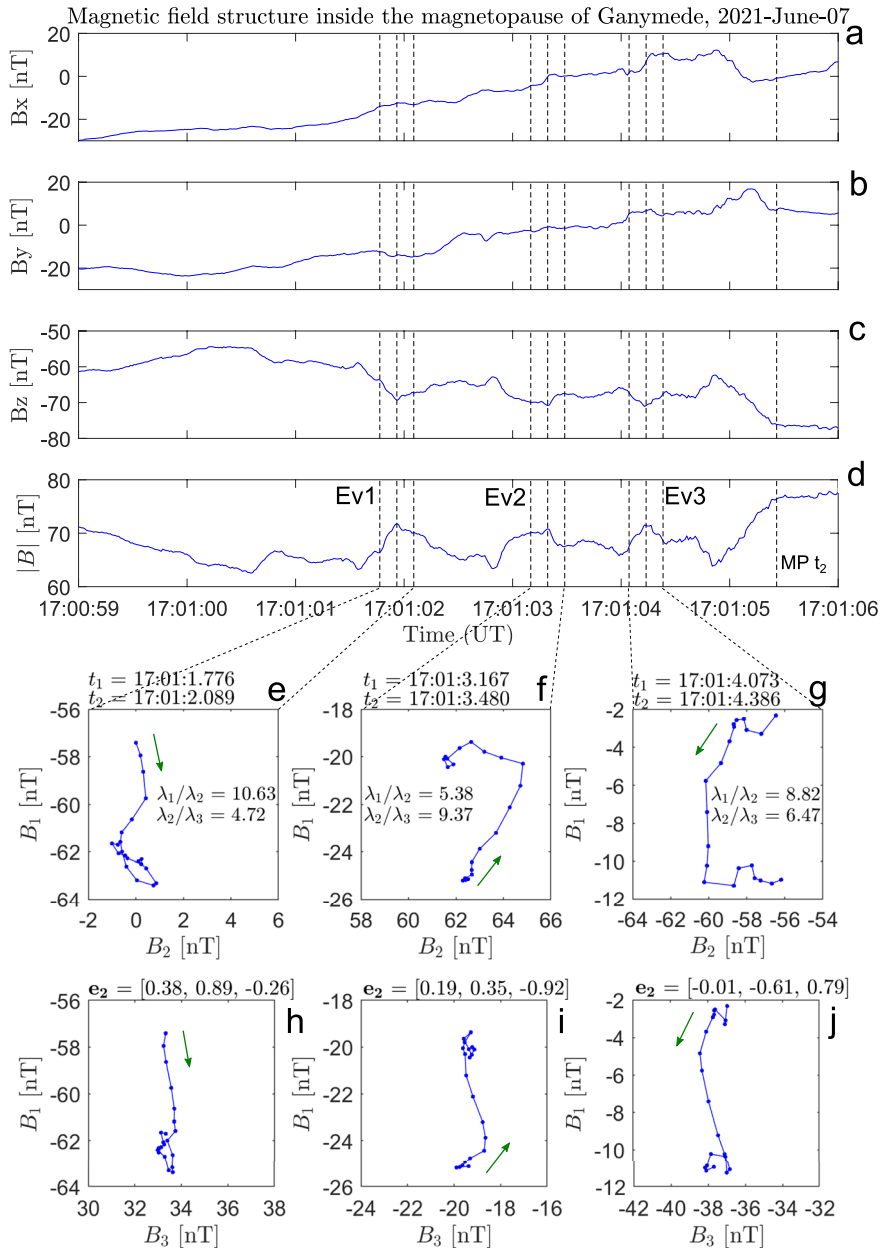

Figure 4. Panels (a–d): Magnetic field Ganymede centered Phi-Omega components and strength observed by Juno Magnetometer, between 17:00:59 and 17:01:06 UT. MP t_2 marks the time Juno ends crossing the magnetopause. Events 1, 2, and 3 (Ev1, Ev2, and Ev3, respectively) are analyzed by minimum variance analysis (MVA). Panels (e–g): B_1 as a function of B_2 for Ev1, Ev2, and Ev3, respectively. Panels (h–j): B_1 as a function of B_3 for Ev1, Ev2, and Ev3, respectively. MVA eigenvalues ratios (λ_1/λ_2 and λ_2/λ_3) and the intermediate variance direction ($\mathbf{e}_2$) are also shown. The green arrows indicate the direction of increasing time.

Jovian-side flank of Ganymede's magnetosphere, near the terminator plane. This time interval displays clear changes in all magnetic field components as the field varied from a Bx/By-dominant configuration in Ganymede's magnetosphere to a Bz-dominated orientation in Jupiter's field. Additionally, we note the presence of quasi-periodic structures near and before MP t_2 (see gray area, Figure 3), analyzed in Figure 4.

We estimate the normal ($\hat{n}$) to the local magnetopause by applying a minimum variance analysis (MVA) to magnetic field observations, between MP t_1 and MP t_2 (Sonnerup & Scheible, 1998). We find $\hat{n}$ is equal to (−0.60, 0.77, 0.19) (in GphiO coordinates), an estimation that is in agreement with expectations based on Galileo MAG observations. Indeed, this vector differs only in ∼6° from (−0.66, 0.75, 0.11), the normal expected based on $f(X$,

Y, *Z*), reported in Kivelson et al. (1998). We also find $f \sim 0.83$, showing this surface function is able to model this magnetopause crossing very well. Indeed, the fit is good when f is close to 1. Analogous results associated with Galileo flybys can be found in Table 3 of Kivelson et al. (1998). MVA maximum to intermediate (λ_1/λ_2) and intermediate to minimum (λ_2/λ_3) eigenvalues ratios are 51.3 and 4.6, respectively, showing the MVA coordinates are well determined for this interval. We therefore compute the angle between $d\mathbf{r}$ (variation of Juno position between MP t_1 and MP t_2) and the observed $\hat{n}$. We find it is ∼2.9° suggesting that, under stationary conditions, Juno's crossing was nearly perpendicular to the local magnetopause surface. We also determine the observed width (along $\hat{n}$) is ∼482 km, that is, on the order of the oxygen Jovian plasma inertial length (∼487 km).

Noticeably, we find evidence for magnetic reconnection in the Juno MAG data. Indeed, the mean value of **B** along $\hat{n}$ (B_n) is 11.67 ± 0.96 nT, where the uncertainty is derived from the MVA analysis (Sonnerup & Scheible, 1998). The presence of a non-zero normal magnetic field component suggests magnetic reconnection was taking place and that the magnetopause was an open, rotational discontinuity, allowing plasma to flow between the Jovian and Ganymede systems. On the contrary, if reconnection was not taking place, this normal magnetic field component would be near zero, and the boundary would be a closed, tangential discontinuity (Sonnerup & Cahill, 1967). The dimensionless reconnection rate can be calculated as the ratio of B_n to the total magnetic field strength right inside the magnetopause, $|\boldsymbol{B}_{GAN}|$ (Sonnerup et al., 1981). We estimate $|\boldsymbol{B}_{GAN}| = 96.21$ nT, based on the mean magnetic field between 17:00:29 UT and MP t_1. As a result, our analysis suggests that the magnetic reconnection rate is equal to ∼0.12 (e.g., DiBraccio et al., 2013; Ebert et al., 2017).

We also estimate the magnetic field shear angle across the magnetopause, as the angle between $\mathbf{B}_{GAN}$ and $\mathbf{B}_{JUP}$. The latter is computed based on the mean magnetic field between MP t_2 and 17:01:15 UT (Figure 3). We find this angle was ∼78.3°. Sonnerup (1974) has reported that reconnection can still occur for relatively small shear angles. This type of component reconnection may take place if the magnetic fields on either side of the magnetopause have the same component parallel to the reconnection X-line (guide field), and the perpendicular components are along the same direction (with the same or opposite sense). In particular, these conditions are satisfied when the magnetic field strength on both sides of the current sheet are comparable, as is the case for Ganymede's upstream magnetopause crossing by Juno (Gosling et al., 2007; Phan et al., 2010). Therefore, the lower shear angle observed along this crossing may be indicative of component reconnection occurring near this location (Sonnerup, 1974). Juno JADE observations near the upstream magnetopause crossing support these results (Ebert et al., 2022). Indeed, the authors reported the presence of heated, counter-streaming electrons near this boundary and conclude the observed signatures constitute evidence for magnetopause reconnection.

Thanks to the fast cadence of the 64 Hz MAG sampling, we are able to identify three short-time scale events occurring within the magnetopause, hereafter referred to as Ev1, Ev2, and Ev3 (Figures 4a–4d). These events were selected based on the local enhancement of the total magnetic field strength (∼10%) and the observed quasi-periodicity, as they could be indicative of a recurrent physical process. To investigate the properties of these events, we apply MVA to the MAG observations of each individual structure. The corresponding time intervals are shown on top of panels (e–g). They are centered on the magnetic field local maximum of each of these events (coincident with the observed inflection point in Bx), and their limits are defined to be able to capture the bipolar signature present in Bx. We determine that 10 measurements before and after the local magnetic field peak are sufficient for this purpose. We find the λ_1/λ_2 and λ_2/λ_3 eigenvalue ratios are greater than or equal to ∼5 for the three events, suggesting the MVA eigenvector basis is well defined. These eigenvectors are orthogonal and represent the directions of maximum ($\mathbf{e}_1$), intermediate ($\mathbf{e}_2$), and minimum variance ($\mathbf{e}_3$) in the magnetic field. The magnetic field components along these eigenvectors are hereafter referred to B_1, B_2, and B_3, respectively.

We conclude that Ev2 and Ev3 are magnetic flux ropes embedded within the magnetopause current sheet. Their signatures follow classic flux rope patterns: a bipolar signature in the B_1 magnetic field component, indicative of the outer helical wraps, and a local maximum of B_2 and $|\mathbf{B}|$ aligning with the bipolar inflection point. This local maximum is representative of the axial-aligned core field of the flux rope (e.g., Bowers et al., 2021; DiBraccio et al., 2015; Elphic et al., 1986; Russell & Elphic, 1979; Slavin et al., 2010, 2012; Trenchi et al., 2016). The bipolar signature for Ev2 ranged from −25.1 to −20 nT while the core field increased by ∼3.3 nT. Analogously, the bipolar signature for Ev3 ranged from −2.3 to −11 nT while the core field increased by ∼4 nT. Figures 4e–4j display hodograms in the maximum-intermediate (B_1-B_2) and maximum-minimum (B_1-B_3) eigenvectors planes, demonstrating the field rotation for each event. We also find that $\mathbf{e}_2$, (shown in panels i–j), forms an angle of 91° and 108° with respect to $\hat{n}$, for Ev2 and Ev3, respectively. Thus, MVA suggests the orientation of these flux

ropes is quasi-perpendicular to the local magnetopause normal, which can be understood in terms of single or multiple X-line reconnection (e.g., DiBraccio et al., 2015; Fear et al., 2007, 2008; Hasegawa et al., 2010; Imber et al., 2011, 2014; Slavin et al., 2012; Trenchi et al., 2011). Indeed, although such orientation is not compatible with elbow-shaped flux tubes (Russell & Elphic, 1979; Varsani et al., 2014), the observed structures can be associated with flux rope models at Earth derived from single (e.g., Fear et al., 2007) and multiple X-line reconnection (e.g., Øieroset et al., 2011). Both crossings (Ev2 and Ev3) did not take place close to the central axis of each flux rope, as evidenced by the fact that B_3 was not close to zero. Given that Juno's speed was on the order of 18.57 km s^{-1}, the observed structures have an apparent size on the order of ∼6 km. MVA results for Ev1 are not conclusive enough to consider this event a flux rope. However, we show them for completeness as this may indeed have been a flux rope in a highly dynamic state.

Detection of flux ropes around Ganymede's magnetopause is of fundamental importance as they affect the plasma environment (storage of magnetic energy and transport of charged particles) and can play a key role in the magnetic field topology reconfiguration. It is also worth emphasizing that flux ropes observed along the dayside magnetopause of other intrinsic magnetospheres are considered to form as by-product of reconnection occurring at a spatially limited reconnection site (Russell & Elphic, 1979), and single or multiple X-lines (see, e.g., Hasegawa et al., 2010; Imber et al., 2011, 2014; Slavin et al., 2012; Trenchi et al., 2011). If either of the last two processes is the origin of the flux ropes observed at Ganymede's upstream magnetopause, their detection further supports the conclusions from our investigation on the (non-zero) mean value of B_n. That is, both analyses suggest magnetic reconnection was occurring along Ganymede's upstream magnetopause.

4. Conclusions

In this work we have analyzed Juno MAG observations during Ganymede's flyby on 7 June 2021. Making use of LatHyS and an analytical model of Ganymede's magnetopause we put into context such observations, and provide predictions for the magnetic field connectivity along the spacecraft trajectory. Our simulation results suggest Juno observed both open and closed magnetic field lines inside Ganymede's magnetosphere. We also characterize the upstream magnetopause properties and determine its location and orientation are consistent with previous Galileo reports. Moreover, we find evidence for magnetic reconnection along Ganymede's upstream magnetopause (see, also, Ebert et al., 2022). Indeed, we find a non-zero magnetic field normal component across the magnetopause and identify flux ropes embedded within the magnetopause current layer. Finally, we estimate a magnetopause reconnection rate of ∼0.12, associated with a shear angle of ∼78.3°.

Data Availability Statement

Juno Magnetometer data are publicly available through the Planetary Data System (https://pds-ppi.igpp.ucla.edu/) at https://doi.org/10.17189/1519711. The LatHyS magnetic field simulation file and the superposition magnetic field profiles can be downloaded from https://figshare.com/s/958dc6b55a9568025b38.

Acknowledgments
The material is based upon work supported by NASA under award number 80GSFC21M0002. R. Modolo is indebted to the "Soleil-Heliosphere-Magnetospheres" program of the French Space Agency CNES for its support. Research at LATMOS has been partly supported by ANR-CNRS through contract ANR-17-CE31-0016. The research at the University of Iowa is supported by NASA through Contract 699041X with Southwest Research Institute. N. Romanelli acknowledges support of the IPSL data center CICLAD.

References

Allegrini, F., Bagenal, F., Ebert, R. W., Louarn, P., McComas, D. J., Szalay, J. R., et al. (2022). Plasma observations during the 7 June 2021 Ganymede flyby from the Jovian Auroral Distributions Experiment (JADE) on Juno. *Geophysical Research Letters*, e2022GL098682. https://doi.org/10.1029/2022GL098682

Bolton, S. J., Lunine, J., Stevenson, D., Connerney, J. E. P., Levin, S., Owen, T. C., et al. (2017). The Juno mission. *Space Science Reviews*, *213*(1–4), 5–37. https://doi.org/10.1007/s11214-017-0429-6

Bowers, C. F., Slavin, J. A., DiBraccio, G. A., Poh, G., Hara, T., Xu, S., & Brain, D. A. (2021). MAVEN survey of magnetic flux rope properties in the Martian ionosphere: Comparison with three types of formation mechanisms. *Geophysical Research Letters*, *48*(10), e2021GL093296. https://doi.org/10.1029/2021GL093296

Carnielli, G., Galand, M., Leblanc, F., Leclercq, L., Modolo, R., Beth, A., et al. (2019). First 3D test particle model of Ganymede's ionosphere. *Icarus*, *330*, 42–59. https://doi.org/10.1016/j.icarus.2019.04.016

Carnielli, G., Galand, M., Leblanc, F., Modolo, R., Beth, A., & Jia, X. (2020a). Constraining Ganymede's neutral and plasma environments through simulations of its ionosphere and Galileo observations. *Icarus*, *343*, 113691. https://doi.org/10.1016/j.icarus.2020.113691

Carnielli, G., Galand, M., Leblanc, F., Modolo, R., Beth, A., & Jia, X. (2020b). Simulations of ion sputtering at Ganymede. *Icarus*, *351*, 113918. https://doi.org/10.1016/j.icarus.2020.113918

Clark, G., Kollmann, P., Mauk, B. H., Paranicas, C., Haggerty, D., Rymer, A., et al. (2022). Energetic charged particle observations during Juno's close flyby of Ganymede. *Geophysical Research Letters*, *49*, e2022GL098572. https://doi.org/10.1029/2022GL098572

Collinson, G., Paterson, W. R., Bard, C., Dorelli, J., Glocer, A., Sarantos, M., & Wilson, R. (2018). New results from Galileo's first flyby of Ganymede: Reconnection-driven flows at the low-latitude magnetopause boundary, crossing the cusp, and icy ionospheric escape. *Geophysical Research Letters*, *45*(8), 3382–3392. https://doi.org/10.1002/2017GL075487

Connerney, J. E. P. (2017). Juno fluxgate magnetometer calibrated data v1.0 [Dataset]. NASA Planetary Data System. https://doi.org/10.17189/1519711

Connerney, J. E. P., Benn, M., Bjarno, J. B., Denver, T., Espley, J., Jorgensen, J. L., et al. (2017). The Juno magnetic field investigation. *Space Science Reviews*, *213*(1–4), 39–138. https://doi.org/10.1007/s11214-017-0334-z

Connerney, J. E. P., Timmins, S., Herceg, M., & Joergensen, J. L. (2020). A Jovian magnetodisc model for the Juno era. *Journal of Geophysical Research: Space Physics*, *125*(10), e2020JA028138. https://doi.org/10.1029/2020JA028138

DiBraccio, G. A., Slavin, J. A., Boardsen, S. A., Anderson, B. J., Korth, H., Zurbuchen, T. H., et al. (2013). MESSENGER observations of magnetopause structure and dynamics at Mercury. *Journal of Geophysical Research: Space Physics*, *118*(3), 997–1008. https://doi.org/10.1002/jgra.50123

DiBraccio, G. A., Slavin, J. A., Imber, S. M., Gershman, D. J., Raines, J. M., Jackman, C. M., et al. (2015). MESSENGER observations of flux ropes in Mercury's magnetotail. *Planetary and Space Science*, *115*, 77–89. https://doi.org/10.1016/j.pss.2014.12.016

Dorelli, J. C., Glocer, A., Collinson, G., & Tóth, G. (2015). The role of the Hall effect in the global structure and dynamics of planetary magnetospheres: Ganymede as a case study. *Journal of Geophysical Research: Space Physics*, *120*(7), 5377–5392. https://doi.org/10.1002/2014JA020951

Dougherty, L. P., Bodisch, K. M., & Bagenal, F. (2017). Survey of Voyager plasma science ions at Jupiter: 2. Heavy ions. *Journal of Geophysical Research: Space Physics*, *122*(8), 8257–8276. https://doi.org/10.1002/2017JA024053

Duling, S., Saur, J., Clark, G., Allegrini, F., Greathouse, T., Gladstone, R., et al. (2022). Ganymede MHD model: Magnetospheric context for Juno's PJ34 flyby. *Geophysical Research Letters*, *49*, e2022GL101688. https://doi.org/10.1029/2022GL101688

Ebert, R. W., Allegrini, F., Bagenal, F., Bolton, S. J., Connerney, J. E. P., Clark, G., et al. (2017). Accelerated flows at Jupiter's magnetopause: Evidence for magnetic reconnection along the dawn flank. *Geophysical Research Letters*, *44*(10), 4401–4409. https://doi.org/10.1002/2016GL072187

Ebert, R. W., Fuselier, S. A., Allegrini, F., Bagenal, F., Bolton, S. J., Clark, G., et al. (2022). Evidence for magnetic reconnection at Ganymede's upstream magnetopause during the PJ34 Juno flyby. *Geophysical Research Letters*, *49*, e2022GL099775. https://doi.org/10.1029/2022GL099775

Elphic, R. C., Cattell, C. A., Takahashi, K., Bame, S. J., & Russell, C. T. (1986). ISEE-1 and 2 observations of magnetic flux ropes in the magnetotail: FTE's in the plasma sheet? *Geophysical Research Letters*, *13*(7), 648–651. https://doi.org/10.1029/GL013i007p00648

Eviatar, A., Vasyliūnas, V. M., & Gurnett, D. A. (2001). The ionosphere of Ganymede. *Planetary and Space Science*, *49*(3), 327–336. https://doi.org/10.1016/S0032-0633(00)00154-9

Fatemi, S., Poppe, A. R., Khurana, K. K., Holmström, M., & Delory, G. T. (2016). On the formation of Ganymede's surface brightness asymmetries: Kinetic simulations of Ganymede's magnetosphere. *Geophysical Research Letters*, *43*(10), 4745–4754. https://doi.org/10.1002/2016GL068363

Fear, R. C., Milan, S. E., Fazakerley, A. N., Lucek, E. A., Cowley, S. W. H., & Dandouras, I. (2008). The azimuthal extent of three flux transfer events. *Annales Geophysicae*, *26*(8), 2353–2369. https://doi.org/10.5194/angeo-26-2353-2008

Fear, R. C., Milan, S. E., Fazakerley, A. N., Owen, C. J., Asikainen, T., Taylor, M. G. G. T., et al. (2007). Motion of flux transfer events: A test of the cooling model. *Annales Geophysicae*, *25*(7), 1669–1690. https://doi.org/10.5194/angeo-25-1669-2007

Gosling, J. T., Phan, T. D., Lin, R. P., & Szabo, A. (2007). Prevalence of magnetic reconnection at small field shear angles in the solar wind. *Geophysical Research Letters*, *34*(15), L15110. https://doi.org/10.1029/2007GL030706

Gurnett, D. A., Kurth, W. S., Roux, A., Bolton, S. J., & Kennel, C. F. (1996). Evidence for a magnetosphere at Ganymede from plasma-wave observations by the Galileo spacecraft. *Nature*, *384*(6609), 535–537. https://doi.org/10.1038/384535a0

Hansen, C. J., Bolton, S., Sulaiman, A. H., Duling, S., Bagenal, F., Brennan, M., et al. (2022). Juno's close encounter with Ganymede - an overview. *Geophysical Research Letters*, *49*, e2022GL099285. https://doi.org/10.1029/2022GL099285

Hasegawa, H., Wang, J., Dunlop, M. W., Pu, Z. Y., Zhang, Q.-H., Lavraud, B., et al. (2010). Evidence for a flux transfer event generated by multiple X-line reconnection at the magnetopause. *Geophysical Research Letters*, *37*(16), L16101. https://doi.org/10.1029/2010GL044219

Imber, S. M., Slavin, J. A., Auster, H. U., & Angelopoulos, V. (2011). A THEMIS survey of flux ropes and traveling compression regions: Location of the near-Earth reconnection site during solar minimum. *Journal of Geophysical Research*, *116*(A2), A02201. https://doi.org/10.1029/2010JA016026

Imber, S. M., Slavin, J. A., Boardsen, S. A., Anderson, B. J., Korth, H., McNutt, R. L., Jr., & Solomon, S. C. (2014). MESSENGER observations of large dayside flux transfer events: Do they drive Mercury's substorm cycle? *Journal of Geophysical Research: Space Physics*, *119*(7), 5613–5623. https://doi.org/10.1002/2014JA019884

Jia, X., & Kivelson, M. G. (2021). The magnetosphere of Ganymede. In *Magnetospheres in the solar system* (pp. 557–573). American Geophysical Union (AGU). https://doi.org/10.1002/9781119815624.ch35

Jia, X., Walker, R. J., Kivelson, M. G., Khurana, K. K., & Linker, J. A. (2008). Three-dimensional MHD simulations of Ganymede's magnetosphere. *Journal of Geophysical Research*, *113*(A6), A06212. https://doi.org/10.1029/2007JA012748

Jia, X., Walker, R. J., Kivelson, M. G., Khurana, K. K., & Linker, J. A. (2010). Dynamics of Ganymede's magnetopause: Intermittent reconnection under steady external conditions. *Journal of Geophysical Research*, *115*(A12), A12202. https://doi.org/10.1029/2010JA015771

Kaweeyanun, N., Masters, A., & Jia, X. (2020). Favorable conditions for magnetic reconnection at Ganymede's upstream magnetopause. *Geophysical Research Letters*, *47*(6), e2019GL086228. https://doi.org/10.1029/2019GL086228

Kim, T. K., Ebert, R. W., Valek, P. W., Allegrini, F., McComas, D. J., Bagenal, F., et al. (2020). Survey of ion properties in Jupiter's plasma sheet: Juno JADE-I observations. *Journal of Geophysical Research: Space Physics*, *125*(4), e2019JA027696. https://doi.org/10.1029/2019JA027696

Kivelson, M. G., Bagenal, F., Kurth, W. S., Neubauer, F. M., Paranicas, C., & Saur, J. (2004). Magnetospheric interactions with satellites. In F. Bagenal, T. E. Dowling, & W. B. McKinnon (Eds.). *Jupiter: The planet, satellites and magnetosphere* (Vol. *1*, pp. 513–536).

Kivelson, M. G., Khurana, K. K., Russell, C. T., Walker, R. J., Warnecke, J., Coroniti, F. V., et al. (1996). Discovery of Ganymede's magnetic field by the Galileo spacecraft. *Nature*, *384*(6609), 537–541. https://doi.org/10.1038/384537a0

Kivelson, M. G., Khurana, K. K., & Volwerk, M. (2002). The permanent and inductive magnetic moments of Ganymede. *Icarus*, *157*(2), 507–522. https://doi.org/10.1006/icar.2002.6834

Kivelson, M. G., Warnecke, J., Bennett, L., Joy, S., Khurana, K. K., Linker, J. A., et al. (1998). Ganymede's magnetosphere: Magnetometer overview. *Journal of Geophysical Research*, *103*(E9), 19963–19972. https://doi.org/10.1029/98JE00227

Kurth, W. S., Sulaiman, A. H., Hospodarsky, G. B., Mauk, B. H., J. M., Clark, G., et al. (2022). Juno plasma wave observations at Ganymede. *Geophysical Research Letters*, e2022GL098591. https://doi.org/10.1029/2022GL098591

Leclercq, L., Modolo, R., Leblanc, F., Hess, S., & Mancini, M. (2016). 3D magnetospheric parallel hybrid multi-grid method applied to planet–plasma interactions. *Journal of Computational Physics*, *309*, 295–313. https://doi.org/10.1016/j.jcp.2016.01.005

Mauk, B. H., Haggerty, D. K., Jaskulek, S. E., Schlemm, C. E., Brown, L. E., Cooper, S. A., et al. (2017). The Jupiter energetic particle detector instrument (JEDI) investigation for the Juno mission. *Space Science Reviews*, *213*(1–4), 289–346. https://doi.org/10.1007/s11214-013-0025-3

McComas, D. J., Alexander, N., Allegrini, F., Bagenal, F., Beebe, C., Clark, G., et al. (2017). The Jovian auroral distributions experiment (JADE) on the Juno mission to Jupiter. *Space Science Reviews*, *213*(1–4), 547–643. https://doi.org/10.1007/s11214-013-9990-9

Modolo, R., Chanteur, G. M., & Dubinin, E. (2012). Dynamic Martian magnetosphere: Transient twist induced by a rotation of the IMF. *Geophysical Research Letters*, *39*(1), L01106. https://doi.org/10.1029/2011GL049895

Modolo, R., Chanteur, G. M., Dubinin, E., & Matthews, A. P. (2005). Influence of the solar EUV flux on the Martian plasma environment. In *Annales Geophysicae*, Copernicus GmbH (Vol. 23, No. (2), pp. 433–444). https://doi.org/10.5194/angeo-23-433-2005

Modolo, R., Chanteur, G. M., Dubinin, E., & Matthews, A. P. (2006). Simulated solar wind plasma interaction with the Martian exosphere: Influence of the solar EUV flux on the bow shock and the magnetic pile-up boundary. In *Annales Geophysicae*, Copernicus GmbH (Vol. 24, No. (12), pp. 3403–3410). https://doi.org/10.5194/angeo-24-3403-2006

Modolo, R., Chanteur, G. M., Wahlund, J.-E., Canu, P., Kurth, W. S., Gurnett, D., et al. (2007). Plasma environment in the wake of titan from hybrid simulation: A case study. *Geophysical Research Letters*, *34*(24), L24S07. https://doi.org/10.1029/2007GL030489

Modolo, R., Hess, S., Génot, V., Leclercq, L., Leblanc, F., Chaufray, J.-Y., et al. (2018). The LatHys database for planetary plasma environment investigations: Overview and a case study of data/model comparisons. *Planetary and Space Science*, *150*, 13–21. (Enabling Open and Interoperable Access to Planetary Science and Heliophysics Databases and Tools). https://doi.org/10.1016/j.pss.2017.02.015

Modolo, R., Hess, S., Mancini, M., Leblanc, F., Chaufray, J.-Y., Brain, D., et al. (2016). Mars-solar wind interaction: LatHys, an improved parallel 3-d multispecies hybrid model. *Journal of Geophysical Research: Space Physics*, *121*(7), 6378–6399. https://doi.org/10.1002/2015JA022324

Øieroset, M., Phan, T. D., Eastwood, J. P., Fujimoto, M., Daughton, W., Shay, M. A., et al. (2011). Direct evidence for a three-dimensional magnetic flux rope flanked by two active magnetic reconnection X lines at Earth's magnetopause. *Physical Review Letters*, *107*(16), 165007. https://doi.org/10.1103/PhysRevLett.107.165007

Paty, C., Paterson, W., & Winglee, R. (2008). Ion energization in Ganymede's magnetosphere: Using multifluid simulations to interpret ion energy spectrograms. *Journal of Geophysical Research*, *113*(A6), A06211. https://doi.org/10.1029/2007JA012848

Paty, C., & Winglee, R. (2004). Multi-fluid simulations of Ganymede's magnetosphere. *Geophysical Research Letters*, *31*(24), L24806. https://doi.org/10.1029/2004GL021220

Paty, C., & Winglee, R. (2006). The role of ion cyclotron motion at Ganymede: Magnetic field morphology and magnetospheric dynamics. *Geophysical Research Letters*, *33*(10), L10106. https://doi.org/10.1029/2005GL025273

Phan, T. D., Gosling, J. T., Paschmann, G., Pasma, C., Drake, J. F., Øieroset, M., et al. (2010). The dependence of magnetic reconnection on plasma β and magnetic shear: Evidence from solar wind observations. *The Astrophysical Journal Letters*, *719*(2), L199–L203. https://doi.org/10.1088/2041-8205/719/2/L199

Richer, E., Modolo, R., Chanteur, G. M., Hess, S., & Leblanc, F. (2012). A global hybrid model for mercury's interaction with the solar wind: Case study of the dipole representation. *Journal of Geophysical Research*, *117*(A10), A10228. https://doi.org/10.1029/2012JA017898

Romanelli, N., DiBraccio, G., Modolo, R., Leblanc, F., Espley, J., Gruesbeck, J., et al. (2019). Recovery timescales of the dayside Martian magnetosphere to IMF variability. *Geophysical Research Letters*, *46*(20), 10977–10986. https://doi.org/10.1029/2019GL084151

Romanelli, N., Modolo, R., Leblanc, F., Chaufray, J.-Y., Hess, S., Brain, D., et al. (2018). Effects of the crustal magnetic fields and changes in the IMF orientation on the magnetosphere of Mars: MAVEN observations and LatHys results. *Journal of Geophysical Research: Space Physics*, *123*(7), 5315–5333. https://doi.org/10.1029/2017JA025155

Romanelli, N., Modolo, R., Leblanc, F., Chaufray, J.-Y., Martinez, A., Ma, Y., et al. (2018). Responses of the Martian magnetosphere to an interplanetary coronal mass ejection: Maven observations and LatHys results. *Geophysical Research Letters*, *45*(16), 7891–7900. https://doi.org/10.1029/2018GL077714

Russell, C. T., & Elphic, R. C. (1979). Observation of magnetic flux ropes in the Venus ionosphere. *Nature*, *279*(5714), 616–618. https://doi.org/10.1038/279616a0

Slavin, J. A., Imber, S. M., Boardsen, S. A., DiBraccio, G. A., Sundberg, T., Sarantos, M., et al. (2012). MESSENGER observations of a flux-transfer-event shower at Mercury. *Journal of Geophysical Research*, *117*(A12), A00M06. https://doi.org/10.1029/2012JA017926

Slavin, J. A., Lepping, R. P., Wu, C.-C., Anderson, B. J., Baker, D. N., Benna, M., et al. (2010). MESSENGER observations of large flux transfer events at Mercury. *Geophysical Research Letters*, *37*(2), L02105. https://doi.org/10.1029/2009GL041485

Sonnerup, B. U. Ö. (1974). Magnetopause reconnection rate. *Journal of Geophysical Research*, *79*(10), 1546–1549. https://doi.org/10.1029/JA079i010p01546

Sonnerup, B. U. Ö., & Cahill, L. J., Jr. (1967). Magnetopause structure and attitude from explorer 12 observations. *Journal of Geophysical Research*, *72*(1), 171–183. https://doi.org/10.1029/JZ072i001p00171

Sonnerup, B. U. Ö., Paschmann, G., Papamastorakis, I., Sckopke, N., Haerendel, G., Bame, S. J., et al. (1981). Evidence for magnetic field reconnection at the Earth's magnetopause. *Journal of Geophysical Research*, *86*(A12), 10049–10067. https://doi.org/10.1029/JA086iA12p10049

Sonnerup, B. U. Ö., & Scheible, M. (1998). Minimum and maximum variance analysis. *ISSI Scientific Reports Series*, *1*, 185–220. Retrieved from http://ftp.issibern.ch/forads/sr-001-08.pdf

Tóth, G., Jia, X., Markidis, S., Peng, I. B., Chen, Y., Daldorff, L. K. S., et al. (2016). Extended magnetohydrodynamics with embedded particle-in-cell simulation of Ganymede's magnetosphere. *Journal of Geophysical Research: Space Physics*, *121*(2), 1273–1293. https://doi.org/10.1002/2015JA021997

Trenchi, L., Fear, R. C., Trattner, K. J., Mihaljcic, B., & Fazakerley, A. N. (2016). A sequence of flux transfer events potentially generated by different generation mechanisms. *Journal of Geophysical Research: Space Physics*, *121*(9), 8624–8639. https://doi.org/10.1002/2016JA022847

Trenchi, L., Marcucci, M. F., Rème, H., Carr, C. M., & Cao, J. B. (2011). TC-1 observations of a flux rope: Generation by multiple X line reconnection. *Journal of Geophysical Research*, *116*(A5), A05202. https://doi.org/10.1029/2010JA015986

Varsani, A., Owen, C. J., Fazakerley, A. N., Forsyth, C., Walsh, A. P., André, M., et al. (2014). Cluster observations of the substructure of a flux transfer event: Analysis of high-time-resolution particle data. *Annales Geophysicae*, *32*(9), 1093–1117. https://doi.org/10.5194/angeo-32-1093-2014

Weber, T., Moore, K., Connerney, J., Espley, J., DiBraccio, G., & Romanelli, N. (2022). Updated spherical harmonic magnetic field moments of Ganymede from the Juno flyby. *Geophysical Research Letters*, *49*, e2022GL098633. https://doi.org/10.1029/2022GL098633

Williams, D. J., Mauk, B. H., McEntire, R. W., Roelof, E. C., Armstrong, T. P., Wilken, B., et al. (1997). Energetic particle signatures at Ganymede: Implications for Ganymede's magnetic field. *Geophysical Research Letters*, *24*(17), 2163–2166. https://doi.org/10.1029/97GL01931

Zhou, H., Tóth, G., Jia, X., & Chen, Y. (2020). Reconnection-driven dynamics at Ganymede's upstream magnetosphere: 3-D global hall MHD and MHD-epic simulations. *Journal of Geophysical Research: Space Physics*, *125*(8), e2020JA028162. https://doi.org/10.1029/2020JA028162